

Damage detection of railway bridges using operational vibration data: theory and experimental verifications

Md Riasat Azim^{1a}, Haiyang Zhang^{2b} and Mustafa Gü^{*3}

¹*Department of Civil & Environmental Engineering, University of Alberta, Natural Resources Engineering Facility 5-090, 9105 116 Street NW, Edmonton, Alberta, T6G 2W2, Canada*

²*Department of Civil & Environmental Engineering, University of Alberta, Natural Resources Engineering Facility 5-042, 9105 116 Street NW, Edmonton, Alberta, T6G 2W2, Canada*

³*Department of Civil & Environmental Engineering, University of Alberta, Donadeo Innovation Centre for Engineering 7-257, 9211 116 Street NW, Edmonton, Alberta, T6G 1H9, Canada*

(Received April 2, 2020, Revised June 1, 2020, Accepted June 2, 2020)

Abstract. This paper presents the results of an experimental investigation on a vibration-based damage identification framework for a steel girder type and a truss bridge based on acceleration responses to operational loading. The method relies on sensor clustering-based time-series analysis of the operational acceleration response of the bridge to the passage of a moving vehicle. The results are presented in terms of Damage Features from each sensor, which are obtained by comparing the actual acceleration response from the sensors to the predicted response from the time-series model. The damage in the bridge is detected by observing the change in damage features of the bridge as structural changes occur in the bridge. The relative severity of the damage can also be quantitatively assessed by observing the magnitude of the changes in the damage features. The experimental results show the potential usefulness of the proposed method for future applications on condition assessment of real-life bridge infrastructures.

Keywords: damage identification; experimental investigation; railway bridges; time-series analysis; operational acceleration response

1. Introduction

Bridges are a critical component of any railway transportation infrastructure network. In addition to approaching the design life span, these bridges are affected by degradation caused by natural disasters like earthquakes and other environmental effects like extreme temperature changes, corrosion, etc. Moreover, these bridges are continuously subjected to increasing operational demand in terms of axle loads and operational frequency. A combination of both natural and human-induced effects could result in degradation of the performance of bridges due to structural damage. If these damages are not detected at a reasonably early stage, it could culminate in the catastrophic failure of bridges. Therefore, it is of utmost importance that these bridge infrastructures are monitored for

*Corresponding author, Associate Professor, E-mail: mustafa.gul@ualberta.ca

^aPh.D. Candidate, E-mail: riasat.azim@ualberta.ca

^bPh.D. Candidate, E-mail: haiyang@ualberta.ca

signs of damage.

Damage detection is a critical component of SHM. In the context of infrastructures, it refers to the identification of the structural changes that could adversely affect the structure. A detailed review of civil infrastructure SHM applications and associated damage detection methods can be found in Brownjohn *et al.* (2004). The condition of bridges is mostly assessed through visual inspections and non-destructive testing, which could be inconsistent in its findings depending on the level of expertise of the investigators. Also, these methods are usually not suitable for continuous monitoring without interrupting bridge operations. Therefore, there is a need for extensive research on developing SHM methods for railway bridges (Moreu *et al.* 2012, Kim *et al.* 2014). Researchers have been focussing on developing various damage detection methods based on vibration data analysis to assist the current on-site inspection strategies. Several researchers have reviewed and developed concepts of damage detections and condition assessment during the past decades for different bridge-type structures. As a result, various SHM concepts based on different parametric and non-parametric damage detection techniques were developed to enhance the existing capabilities for condition assessment of bridges (for example, Meherjo *et al.* 2008, Scianna and Christenson 2009, Lu and Liu 2011, Moaveni *et al.* 2012, Catbas *et al.* 2012, Scott *et al.* 2013, You *et al.* 2015, Sadhu *et al.* 2015, etc.).

Most of the researchers working on the SHM of railway bridges have focused on the numerical and experimental simulation of girder and truss bridges. In 2012, a wavelet transformation-based damage detection method was proposed by Beskyroun *et al.* (2010). They used the dynamic response of a steel railway bridge to actuator-applied excitation as the data for wavelet transformation. In their study, the damage is detected by comparing the damage indicator under baseline and damaged conditions. While the methodology is successful in detecting and locating damage, it is not suitable for continuous maintenance under operational conditions. A train induced bridge acceleration response-based damage detection method has been developed by (Zhan *et al.* 2011). The researchers demonstrated damage identification in terms of response sensitivity matrices which are updated using an iterative procedure to locate and quantify the damage in railway bridges. The method compares the existing bridge response to the damaged response and can detect and locate damage to the bridge. It is only effective when the same train at the same speed is used for measuring the response at the undamaged and damaged state. Bowe *et al.* (2015) proposed a damage detection method using the analysis of vehicle accelerations resulting from the train-track-bridge interaction. The response was obtained from accelerometers mounted on the train itself. Using a wavelet transform-based technique, this method can detect and locate the damage in terms of the change in pseudo frequency. However, the method is not as efficient in the presence of noise. In another study, a damage detection strategy for railway bridges based on artificial neural networks (ANN) was developed by Gonzalez and Karoumi (2015). The study used bridge acceleration data as the primary input and proposed a damage indicator based on the prediction error of the ANN system. However, one limitation of their study is that a simply supported beam is represented as a railway bridge while a real-life railway bridge is a complex structure. The method is also limited in the sense that, to ensure accuracy, the train load's position and speed need to be known by the bridge weigh-in-motion system. Moreu *et al.* (2015) conducted extensive tests on real-life timber railway bridges and collected vertical and transverse displacements. The study suggested that transverse displacement could assist in the condition assessment of railway bridges. However, displacement values are affected by train speed, direction, and train-track-bridge interaction in addition to structural changes. Therefore, the presence of damage and its location, may not be discernible using the analysis of operational displacement data. Farahani and Penumado (2016) proposed a damage

feature based on the ratio of the standard deviation of the prediction error of the damaged bridge to the healthy bridge. This method used velocity response to impact loading on a steel girder bridge. While the methodology is encouraging, damage localization is still an issue, especially when data is contaminated by noise. George *et al.* (2017) discussed an energy-based method to detect damage in train under train traffic load by comparing the normalized signal energies of the vertical acceleration response of the healthy and damaged bridge. At present, the method is only able to detect the presence of damage. Various other damage detection methods for girder and truss bridges have been presented in the literature (examples include research conducted by Kopsaftopoulos and Fassois, 2010, Wang *et al.* 2012, Kim *et al.* 2014, Siriwardena 2015, Azim and Güл 2020a, b, etc.).

It is acknowledged that major improvements have indeed occurred towards developing useful vibration-based health monitoring strategies for railway bridges in recent years. However, most of these methods are successful in identifying the existence of damage which is level 1 damage detection according to Rytter (1993). These do not completely address the issues such as detecting and locating local damage (Level 2 damage detection), countering the effects of noisy data exhibiting false positive or negative damage, and accounting for operational variability. This is not adequate for bridge monitoring considering that bridges (especially truss bridges) usually have too many elements and information on the location of the damage is important. The authors in their previous studies have utilized times series analysis and proposed acceleration-based methods which are shown to be effective in identifying and locating damage in various types of structures (Mei and Güл 2014, Celik *et al.* 2018, Do *et al.* 2019). For girder and truss railway bridges, the authors have proposed a damage detection method using sensor clustering-based time series analysis where ARMAX models were used to fit acceleration response from multiple sensor clusters for localizing and relatively assessing the severity of damage due to stiffness loss with numerical applications only (Azim and Güл 2019, Azim and Güл 2020). The major advantage of the proposed method is the ability to detect and locate damage in girder and truss elements using operational acceleration data.

This paper could be considered as a subsequent study of the previous works of the authors (Azim and Güл 2019, Azim and Güл 2020c). In this paper, the results of experimental studies conducted on two bridge prototypes under the laboratory environment are presented. The goal of this study is to demonstrate the performance of the above-proposed method on experimental bridge prototypes. Two experimental bridges are fabricated. The first bridge is a simple steel deck bridge and the next one is a timber truss bridge with a steel deck. Through the experimental results, it is shown that the proposed method can be effective in assessing damage under a laboratory environment.

2. Theoretical background

The dynamic responses (accelerations, velocities, and displacements) of a structure are governed by the equation of motion (EOM). This equation, with which the linear dynamic response of a structure with N Degrees of Freedoms (DOFs) complies with can be written in simple form as Eq. (1). Here, \mathbf{M} , \mathbf{C} , \mathbf{K} represent mass, damping, and stiffness matrices of the system, respectively. The vectors, \mathbf{u} , $\dot{\mathbf{u}}$, $\ddot{\mathbf{u}}$ are displacements, velocities, and accelerations, respectively. The external forcing function is denoted by \mathbf{P} . If the free response is considered, Eq. (1) can be simplified to obtain a response for the 1st DOF of an N DOF system, \ddot{u}_1 as in Eq. (3).

$$\mathbf{M}\ddot{\mathbf{u}}(\mathbf{t}) + \mathbf{C}\dot{\mathbf{u}}(\mathbf{t}) + \mathbf{K}\mathbf{u}(\mathbf{t}) = \mathbf{P}(\mathbf{t}) \quad (1)$$

$$m_{ii}\ddot{u}_i(t) + \dots + m_{iN}\ddot{u}_N(t) + c_{ii}\dot{u}_i(t) + \dots + c_{iN}\dot{u}_N(t) + k_{ii}u_i(t) + \dots + k_{iN}u_N(t) = 0 \quad (2)$$

Eq. (2) contains velocity and displacement terms. The time-series model used in the study only incorporates acceleration response since in real-life bridges, obtaining velocity and displacement responses under a moving train can be very difficult. Therefore, the central difference technique is implemented in the 2nd derivative of Eq. (2) to replace the velocity and displacement terms leaving Eq. (2) with acceleration response only. Then finally rearranging, Eq. (3) is obtained. The detailed derivation of the method is presented in the authors' previous work (Azim and Güл 2019).

$$\left(\frac{m_{ii}}{(\Delta t)^2} + \frac{c_{ii}}{2\Delta t} \right) \ddot{u}_i(t + \Delta t) = \left\{ \begin{array}{l} - \sum_{j=1, j \neq i}^N \left(\frac{m_{jj}}{(\Delta t)^2} + \frac{c_{jj}}{2\Delta t} \right) \ddot{u}_j(t + \Delta t) \\ + \sum_{j=1}^N \left(\frac{2m_{ij}}{(\Delta t)^2} - k_{ij} \right) \ddot{u}_j(t) + \sum_{j=1}^N \left(-\frac{m_{jj}}{(\Delta t)^2} + \frac{c_{jj}}{2\Delta t} \right) \ddot{u}_j(t - \Delta t) \end{array} \right\} \quad (3)$$

Rewriting Eq. (3) for $\ddot{u}_i(t)$ by subtracting Δt from acceleration components on both sides of the Eq. (3), finally Eq. (4) is obtained. It can be seen that, for the i^{th} DOF, the sum of j^{th} DOFs is the contribution from adjacent DOFs which includes the i^{th} DOF itself for the $(t - \Delta t)$ and the $(t - 2\Delta t)$ time-steps.

$$\ddot{u}_i(t) = \frac{1}{\left(\frac{m_{ii}}{(\Delta t)^2} + \frac{c_{ii}}{2\Delta t} \right)} \left\{ \begin{array}{l} - \sum_{j=1:N, j \neq i} \left(\frac{m_{jj}}{(\Delta t)^2} + \frac{c_{jj}}{2\Delta t} \right) \ddot{u}_j(t) \\ + \sum_{j=1:N} \left(\frac{2m_{ij}}{(\Delta t)^2} - k_{ij} \right) \ddot{u}_j(t - \Delta t) + \sum_{j=1:N} \left(-\frac{m_{ij}}{(\Delta t)^2} + \frac{c_{ij}}{2\Delta t} \right) \ddot{u}_j(t - 2\Delta t) \end{array} \right\} \quad (4)$$

Therefore, a model could be generated to predict the output of the i^{th} DOF by using the DOFs adjacent to it. Similar equations can be written for each row and different models can be created for each DOF of the structure. Each row of Eq. (4) can be considered as a sensor cluster with a reference DOF and its adjacent DOFs. Therefore, different linear time series models can be created to establish different models for each sensor cluster and changes in these models can indicate the presence of damage along with its location and severity. In this study, time series models are used to fit the above dynamic response of a structure. The Auto-Regressive Moving Average with eXogenous (ARMAX) input time series model to represent the relationship between input, output, and error terms of a system can be written as Eq. (5)

$$\begin{aligned} y(t) &+ a_1 y(t - \Delta t) + \dots + a_{n_a} y(t - n_a \Delta t) \\ &= b_1 x(t - \Delta t) + \dots + b_{n_b} x(t - n_b \Delta t) + e(t) + d_1 e(t - \Delta t) + \dots + d_{n_d} e(t - n_d \Delta t) \end{aligned} \quad (5)$$

where $y(t)$, $x(t)$, and $e(t)$ are output, input, and error terms of the model, respectively. The unknown parameters of the model are shown with a_i , b_i , and d_i . The model orders are n_a , n_b , and n_d . By changing

the model orders, different time-series models can be defined.

In this study, time series model parameters are obtained by the least square error method. Model orders are obtained by observing the delay in input and output terms in Eq. (4) and are set as 0 for n_a and 2 for n_b . Based on these, the final form of ARMAX mode for the proposed methodology can be obtained as shown in Eq. (6).

$$\ddot{u}_i(t) = \left\{ \begin{array}{l} b_{i,1}^1 \ddot{u}_1(t) + \cdots + b_{i,i-1}^1 \ddot{u}_i(t) + b_{i,i+1}^1 \ddot{u}_{i+1}(t) + \cdots + b_{i,N}^1 \ddot{u}_N(t) \\ + b_{i,1}^2 \ddot{u}_1(t - \Delta t) + \cdots + b_{i,N}^2 \ddot{u}_N(t - \Delta t) \\ + b_{i,1}^3 \ddot{u}_1(t - 2\Delta t) + \cdots + b_{i,N}^3 \ddot{u}_N(t - 2\Delta t) + e(t) + d_1 e(t - \Delta t) + \cdots + d_{n_d} e(t - n_d \Delta t) \end{array} \right\} \quad (6)$$

Eq. (6) is used to create different sensor clusters. These models can then be used to extract damage related features to identify, locate, and estimate the relative severity of the damage. After creating the ARMAX models for both healthy and damaged condition utilizing the sensor clustering framework, Damage Features (DFs) are extracted from the ARMAX models. For this study, DF is defined as the difference between Fit Ratios (FR). FR is expressed as a normalized root mean squared error as shown in Eq. (7) where y_m , y_p , and \underline{y}_m are measured output, predicted output, and mean of measured output data, respectively.

$$FR = \left(1 - \frac{\|y_m - y_p\|}{\|y_m - \underline{y}_m\|} \right) \quad (7)$$

The DF is calculated using Eq. (8). Here, FR_1 is the fit ratio of the actual response to the predicted response from the ARMAX model for the damaged bridge. FR_2 is the fit ratio obtained by fitting the damaged actual response to the predicted baseline response from the ARMAX model. When the structure is damaged, the ARMAX model based on baseline data cannot fit the damaged data adequately enough compared to the ARMAX models based on damaged data due to the changes in the structural properties. Therefore, by comparing the differences in values of DFs between different DOFs, the presence of damage, its location, and relative severity can be assessed.

$$DF = \frac{|FR_1 - FR_2|}{FR_1} \times 100 \quad (8)$$

3. Experimental validation on a simple deck bridge

As part of our experimental investigation plan to validate the proposed method, a simply supported slab bridge is considered as shown in Figure 1. The bridge deck is made of hot rolled steel W44, which has a yield strength of 250 MPa and ultimate strength of 310 MPa. The modulus of elasticity of the steel is 200 GPa. The dimensions of the bridge are as follows: length of 2000mm, width of 330 mm, and thickness of 6.35 mm. The bridge is instrumented with three tri-axial wireless accelerometers (Brand: Lord Microstrain Sensing (2019), Model: G-Link-200) denoted as N1, N2,

and N3 in Fig. 1. These are placed at 1/4th, mid-span, and 3/4th span along the direction of travel. Two artificial damage cases are considered. A moving vehicle is used to generate vertical accelerations data from the sensors. The vertical acceleration response is collected at a frequency of 512 Hz. The vehicle is shown in Figure 2. The vehicle is controlled by a motor. By adjusting the power transmitted to the motor, the speed of the vehicle can be changed. The sensor cluster system is presented in Table 1. Each sensor cluster consists of a reference channel (whose output is predicted) and its adjacent channels (which are used as inputs to predict the output of the reference channel). As discussed in the theoretical derivation section, the adjacent channels to each reference channel, include the reference channel itself. For example, the output of N2 is predicted from inputs from adjacent channels N1, and N3 as well as the N2 channel itself (based on the Eq. (4)) which together forms one cluster. For this bridge, there are 3 cluster systems.

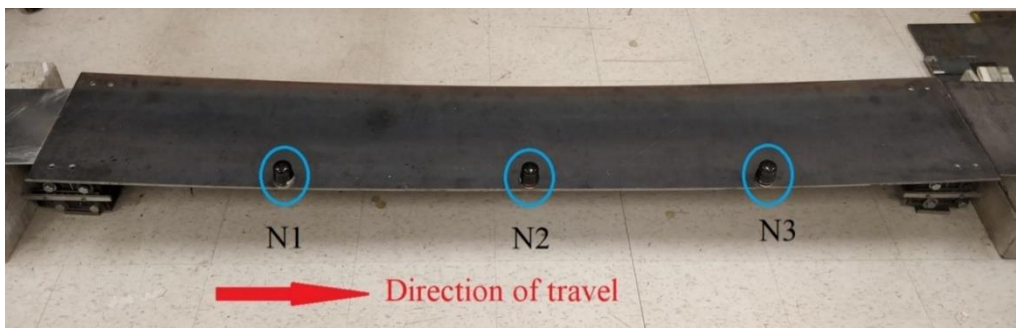


Fig. 1 Experimental Setup for the simple bridge under baseline condition



Fig. 2 Vehicle to induce vibration in the bridge

Table 1 Sensor clusters for the simple deck bridge

Output of the ARMAX model (Reference channel)	Inputs to the ARMAX model (Adjacent channels+ Reference channel)
N1	N1, N2
N2	N1, N2, N3
N3	N2, N3

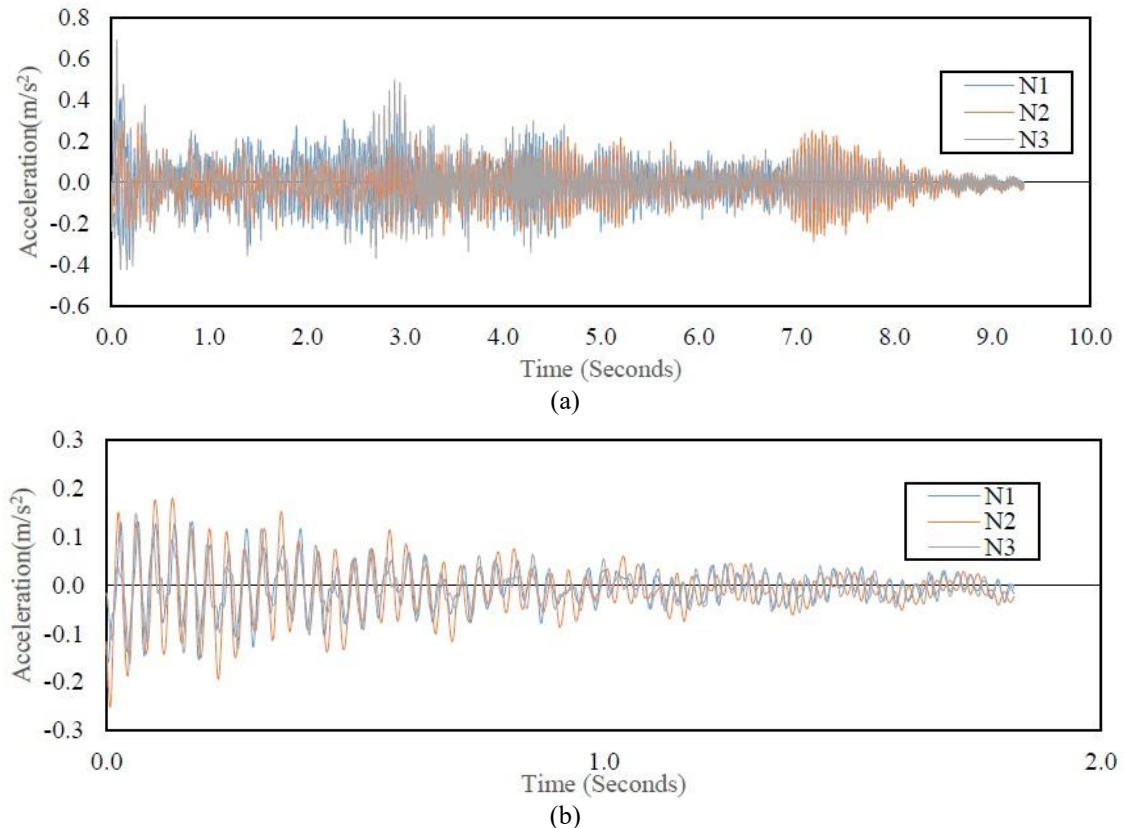


Fig. 3 Acceleration response of the bridge from the instrumented nodes (a) total response (b) free response after the vehicle passage

3.1 Threshold estimation

Initially, the two different configurations of the vehicle are passed over the baseline bridge several times. The 1st configuration (Vehicle-1) weighs around 2.5 kg and passed over the bridge at an average speed of 0.25 m/s. The 2nd configuration (Vehicle-2) weighs around 3.0 kg and passed over the bridge at an average speed of 0.35 m/s. After obtaining the total response, the initial free vibration portion of the data when the vehicle is off the bridge are extracted from each experiment. Some sample data for the baseline bridge due to the passage of Vehicle-1 is shown in Fig. 3.

To estimate the threshold DF, considering the operational variation, one set of baseline data from Vehicle-1 is compared with 5 sets of baseline data from Vehicle-2. These data sets are then analyzed by the proposed sensor clustering-based method. Then fit ratios are obtained by comparing the measured data to the predicted data from the method. This results in five different FRs and therefore, five different DFs from each of three accelerometers for the baseline bridge. Finally, the maximum DF among these 15 DFs is considered as the threshold damage feature which in this experimental investigation is found to be 5.40. So, any DF value above 5.40 is expected to imply structural change.

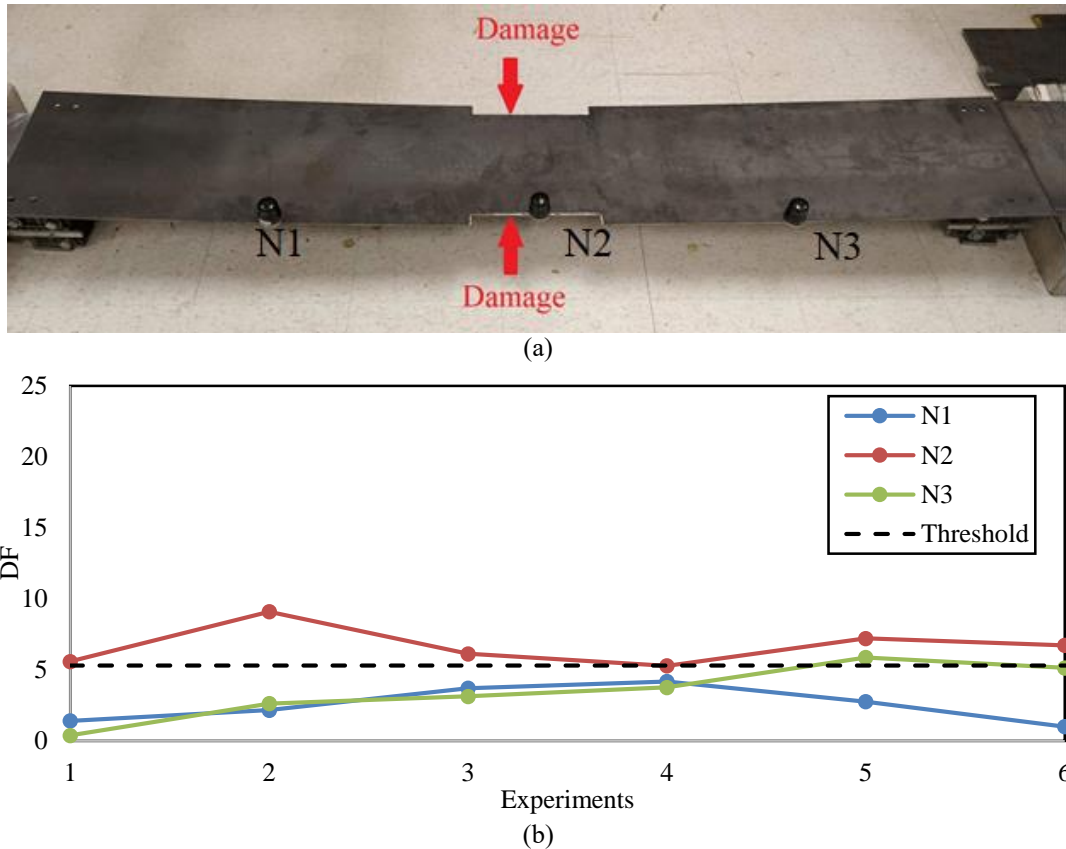


Fig. 4 (a) Damage case DC-1 and (b) Damage Features for DC-1

3.2 Damage investigation

Two damage cases are considered for experimental validation of the proposed method for the simple deck bridge. These are, DC-1: 15% reduction in the cross-sectional area centered at the mid-span, and DC-2: 30% reduction in the cross-sectional area centered at the 1/4th span along the direction of travel. The results for these two damage cases are discussed in sections 3.2.1 and 3.2.2, respectively.

3.2.1 Damage features for DC-1: 15% reduction in the cross-sectional area centered at the mid-span

In this damage case, the bridge has a 24.8 mm by 250 mm cut centered at the mid-span at each side as shown in Fig. 4(a) so that there is a 15% loss in the cross-sectional area. Vehicle-2 is passed over this damaged bridge six times and free acceleration responses are extracted. The analysis results for this damage case are shown in Figure 4(b) in which the damaged bridge responses from Vehicle-2 are compared with the Vehicle-1 data used during threshold estimation. As seen in Fig. 4(b), maximum DFs are obtained for N2 (located at the mid-span) with average values of 6.70. The other

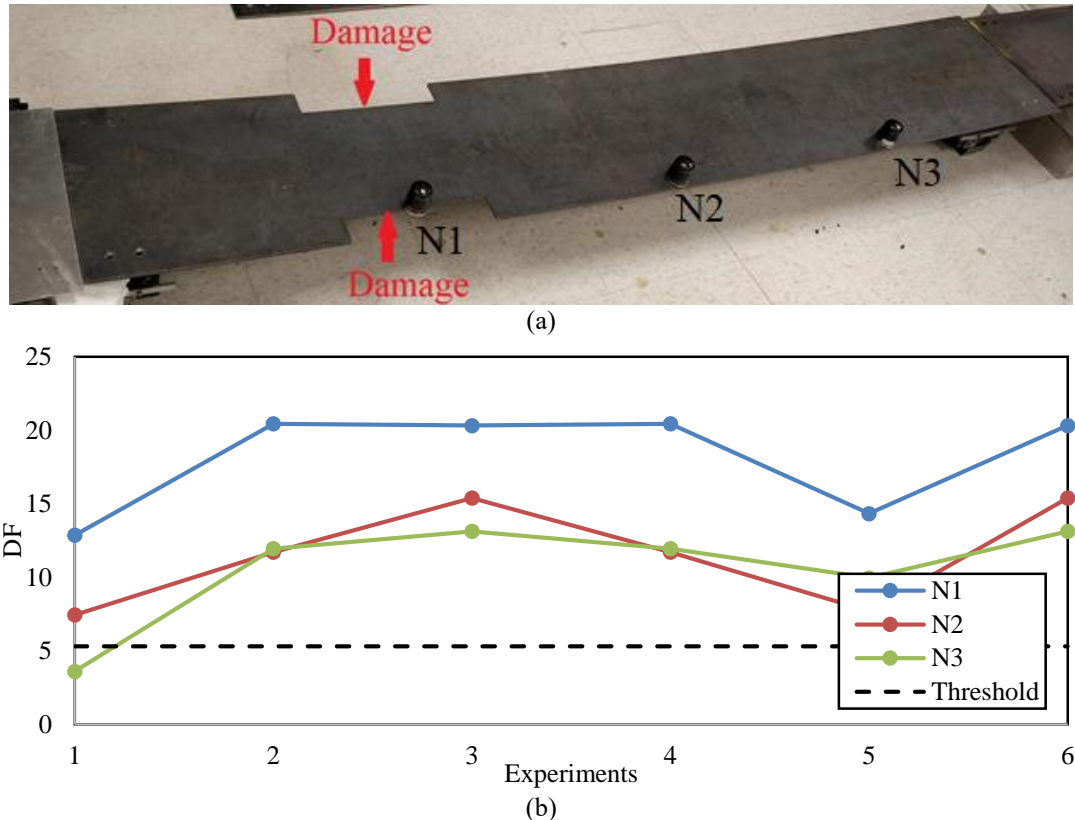


Fig. 5 (a) Damage case DC-2 and (b) Damage features for DC-2

nodes N1 and N3 show average DFs of 2.5 and 3.5, respectively which are below the threshold value of 5.4. Based on the values of DFs, it is indicative that damage is present with a likely location around the mid-span.

It is noted that there are some variations in DFs between experiments. For example, for N2, the maximum DF is 9.1 for experiment 2 and the minimum is 5.3 for experiment 4. The speed of the vehicle varied while passing over the bridge due to the curvature of the deck. Besides, the travel paths of the vehicle between experiments were not the same. These two issues could have affected the free response of the bridge apart from the actual presence of damage.

3.2.2 Damage features for DC-2: 30% reduction in the cross-sectional area centered at the 1/4th span along the direction of travel

In this damage case, the bridge has a 49.5 mm by 250 mm cut near the 1/4th span as shown in Fig. 5(a) so that there is a 30% loss in the cross-sectional area centered at the 1/4th span. Similar to the previous damage case, Vehicle-2 is passed over this damaged bridge six times and the acceleration response is obtained. The results analyzing this damage case are shown in Fig. 5(b). As seen in Fig. 5(b), maximum DFs are obtained for N1 (located near approach span) with average values of 18.1. The other nodes N1 and N3 show average DFs of 11.6 and 10.6, respectively. Based

on the values of DFs, it is indicative that damage is present with a likely location near the sensor installed closer to the approach span, which is consistent with the applied damage. Also, by comparing the DFs of this damage case with the previous one, it is seen that the DFs are more than two times higher in this case. The average DFs of all the nodes are above the threshold. This is likely because this severe damage caused some load re-distribution over the entire bridge. The variations between DFs could be attributed to the same reasons discussed in the previous damage case.

4. Experimental validation on a truss bridge prototype

The second experimental setup includes a simply supported truss bridge prototype as shown in Fig. 6. The total span of the truss is 2 m. The truss elements are cut into rectangular cross-sections from SPF (Spruce, pine, and fir) dimension lumber pieces. These are timber pieces made up of Spruce, Pine, and Fir woods. The pieces used in this research are graded as “No.2” which are suitable for engineering applications such as trusses according to the Canadian Wood Council (CWC 2020). The material has a modulus of elasticity of around 8.5 GPa. The dimensions and cross-sectional properties are presented in Table 2. The truss elements are bolted to the gusset plates made of same dimension lumber pieces using 6.35 mm diameter steel bolts. The bridge deck is made of hot rolled steel W44, which has the modulus of elasticity of is 200 GPa. The dimensions of the bridge are as follows: 2 m length, 330 mm width, and 6.35 mm thickness.



Fig. 6 Experimental Setup for the truss bridge under baseline condition

Table 2 Truss element section properties

Truss element	Length (mm)	Width (mm)	Thickness (mm)
Top and Bottom Chord	500	25	12
Verticals	300	25	12
Diagonals	580	25	12
Cross bracings	350	25	25

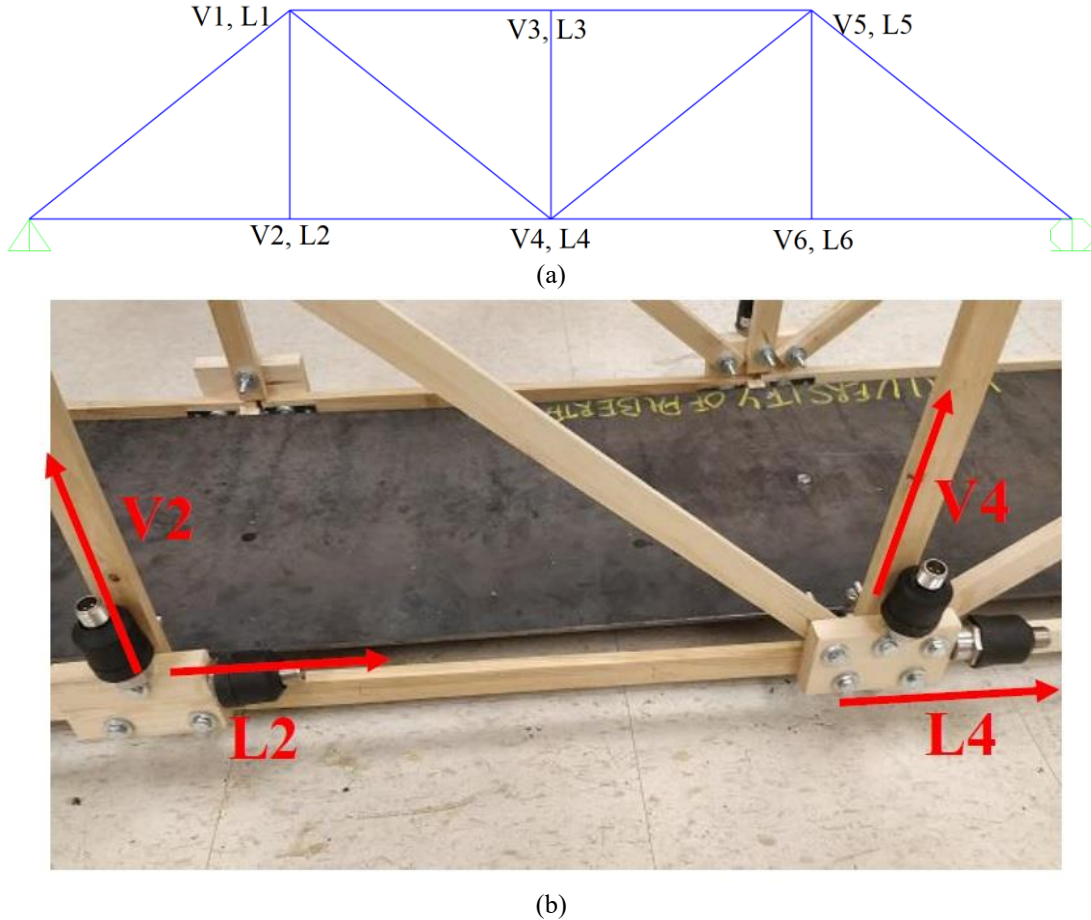


Fig. 7 (a) Schematic diagram showing the instrumentation of the truss bridge and (b) Enlarged view of the sensors V2-L2 on the actual bridge

To validate the proposed method, one side of the truss bridge is instrumented with uniaxial accelerometers. At each connection, two accelerometers are placed to collect acceleration response in both vertical and longitudinal directions as shown in Figs. 7(a) and 7(b). Therefore, in total 12 uniaxial accelerometers (Brand: PCB Piezotronics (2019), Model: 393A03) are placed on one side of the truss bridge. Instrumenting with 12 accelerometers on one side of the truss does add some mass to the bridge on that side. However, it does not cause any stability issues for the truss bridge. Since the same instrumentation setup is used for both baseline and damaged bridge, there is no change in mass due to instrumentation between experiments. The change in mass between experiments is only due to the replacement of original truss elements with damaged elements.

These accelerometers are designated according to the vertical and longitudinal direction ('V' and 'L', respectively). The vertical and longitudinal cluster systems are formulated based on the assumption that the vertical cluster would identify damage in vertical truss elements while the longitudinal cluster would identify damage in the elements aligned in the longitudinal direction.

Table 3 Sensor clusters for the truss bridge

Vertical Sensor Clusters		Longitudinal Sensor Clusters	
Output of the ARMAX model (Reference channel)	Inputs to the ARMAX model (Adjacent channels+ Reference channel)	Output of the ARMAX model (Reference channel)	Inputs to the ARMAX model (Adjacent channels+ Reference channel)
V1	V1, V2, V4	L1	L1, L3, L4
V2	V1, V2	L2	L2, L4
V3	V3, V4	L3	L1, L3, L5
V4	V1, V3, V4, V5	L4	L1, L2, L4, L5, L6
V5	V4, V5, V6	L5	L3, L4, L5
V6	V5, V6	L6	L4, L6

The vertical and longitudinal sensor cluster systems are presented in Table 3. Similar to the example presented for the steel deck bridge, each sensor cluster consists of a reference channel (whose output is predicted) and its adjacent channels (which are used as inputs to predict the output of the reference channel). Since the output of the reference channels also depends on the input from the reference channel, the reference channel is included as part of the adjacent channels that form the sensor cluster system. In this truss bridge, for example, the output of vertical sensor V1 is predicted from the inputs of V1, V2, and V4. V1 is the output channel itself which is also included as input. V2 and V4 are adjacent channels to V1 which are vertically and diagonally connected to V1. Similarly, the output of longitudinal sensor L1 is predicted from the inputs of L1, L3, and L4. L1 is the output channel itself which is also included as input. L3 and L4 are adjacent channels to L1 which are longitudinally and diagonally connected to L1.

4.1 Threshold estimation

Initially, the vehicle is passed over the baseline truss bridge several times as shown in Fig. 8 to obtain a few sets of baseline data which include the vibration response during the passage of the vehicle and a few seconds of free vibration response. To incorporate variation in vehicle load and speed, two-vehicle weight and speed combinations are considered. The 1st configuration is Vehicle-1 weighing 3.5 kg moving at an average speed of 0.35 m/s. The 2nd configuration is Vehicle-2 weighing 5.0 kg moving at an average speed of 0.25 m/s.

To estimate threshold DFs, one set of baseline data in response to Vehicle-1 is compared with five sets of baseline data in response to Vehicle-2. For both types of vehicle passage, data sets are collected at a frequency of 2048 Hz. These data sets are then analyzed by the sensor clustering-based proposed method. Then fit ratios are obtained by comparing the actual data to the predicted response from the method for both vertical and longitudinal cluster. Finally, the maximum difference of fit ratios among the five different experiments is calculated as the threshold damage feature which in this experimental investigation is found to be 5.89 and 2.07 for vertical cluster and longitudinal cluster, respectively. So, any DF values above these thresholds are expected to imply structural changes that affect the corresponding cluster.



Fig. 8 Vehicle passing over the truss bridge deck

4.2 Damage investigation

To validate the proposed damage detection method for the truss bridge, two damage cases are investigated. These are, DC-A: 33% thickness loss in vertical element between nodes 1 and 2, and DC-B: 33% thickness loss in longitudinal element between nodes 2 and 4.

The results for these two damage cases are discussed in the subsequent paragraphs. The results for the damage cases are presented when baseline data in response to the passage of Vehicle-1 is compared with damaged bridge data in response to Vehicle-2.

4.2.1 Damage features for DC-A: 33% thickness loss in vertical element between nodes 1 and 2

In this damage case, the vertical truss element between nodes 1 and 2 is damaged by reducing its thickness from 12 mm to 8 mm resulting in a 33% reduction in cross-sectional area and consequently axial stiffness. The Damage Feature (DFs) for the case are shown in Fig. 9 where (a) and (b) represent results from the vertical and longitudinal clusters, respectively. From vertical cluster analysis, the average DF for V1 is around 31.4 which is almost 3 times higher than the threshold. The average DF for V2 is around 12.2 which is also higher than the threshold. The longitudinal clusters show that all the DFs are very close to or below the threshold indicating that no damage likely in the longitudinal direction. Overall, by observing the DFs of both vertical and longitudinal clusters, it can be inferred that damage is present and its likely location is in the vertical members between nodes V1 and V2. The results also show that the method can detect and locate damage in the vertical element.

4.2.2 Damage features for DC-B: 33% thickness loss in longitudinal element between nodes 2 and 4

In this damage case, the longitudinal truss element between nodes 2 and 4 is damaged by reducing the cross-sectional thickness by 33%. The Damage Features (DFs) for this case are shown in Fig. 10

where (a) and (b) represent results from the vertical and longitudinal clusters, respectively. It can be observed that the average DFs for vertical clusters are all very close to or below the threshold value indicating that no damage is likely in the vertical system. In the longitudinal system, the highest DFs are obtained for L2 and L4 with average values of 3.6 and 3.2, respectively. The average DFs for the rest of the nodes are below the threshold. This is indicative of the fact that damage is present, and its likely location is in the longitudinal truss element between nodes 2 and 4 with no damage occurred elsewhere.

Fabrication error resulted in differences in elevations between nodes that otherwise are supposed to be aligned longitudinally. Similar to the slab bridge, the speed of the vehicles varied while passing over the truss bridge and between experiments due to the curvature of the deck. Besides, the travel paths of the vehicle between experiments were not always similar. These issues might have influenced the free vibration response apart from the damage itself, which resulted in the variation of DFs between experiments.

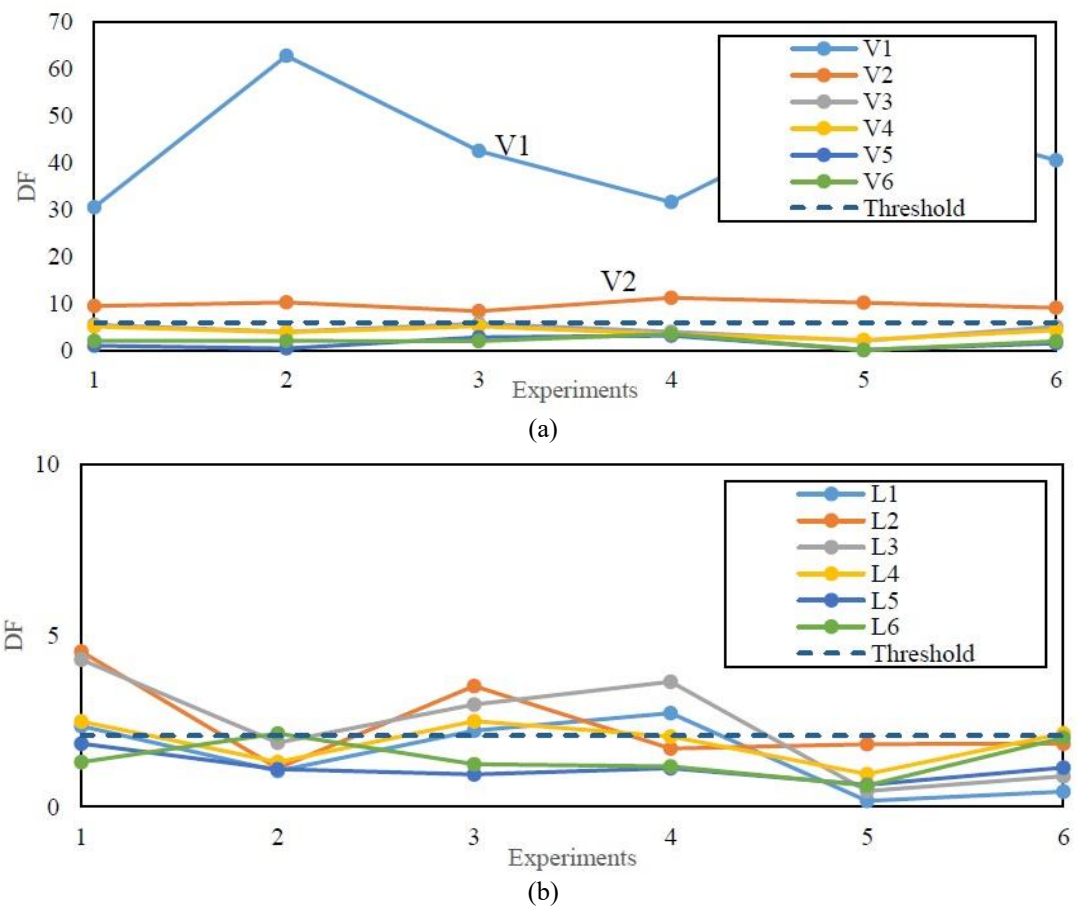


Fig. 9 Damage Features (DFs) for DC-A: (a) Vertical Cluster and (b) Longitudinal Cluster

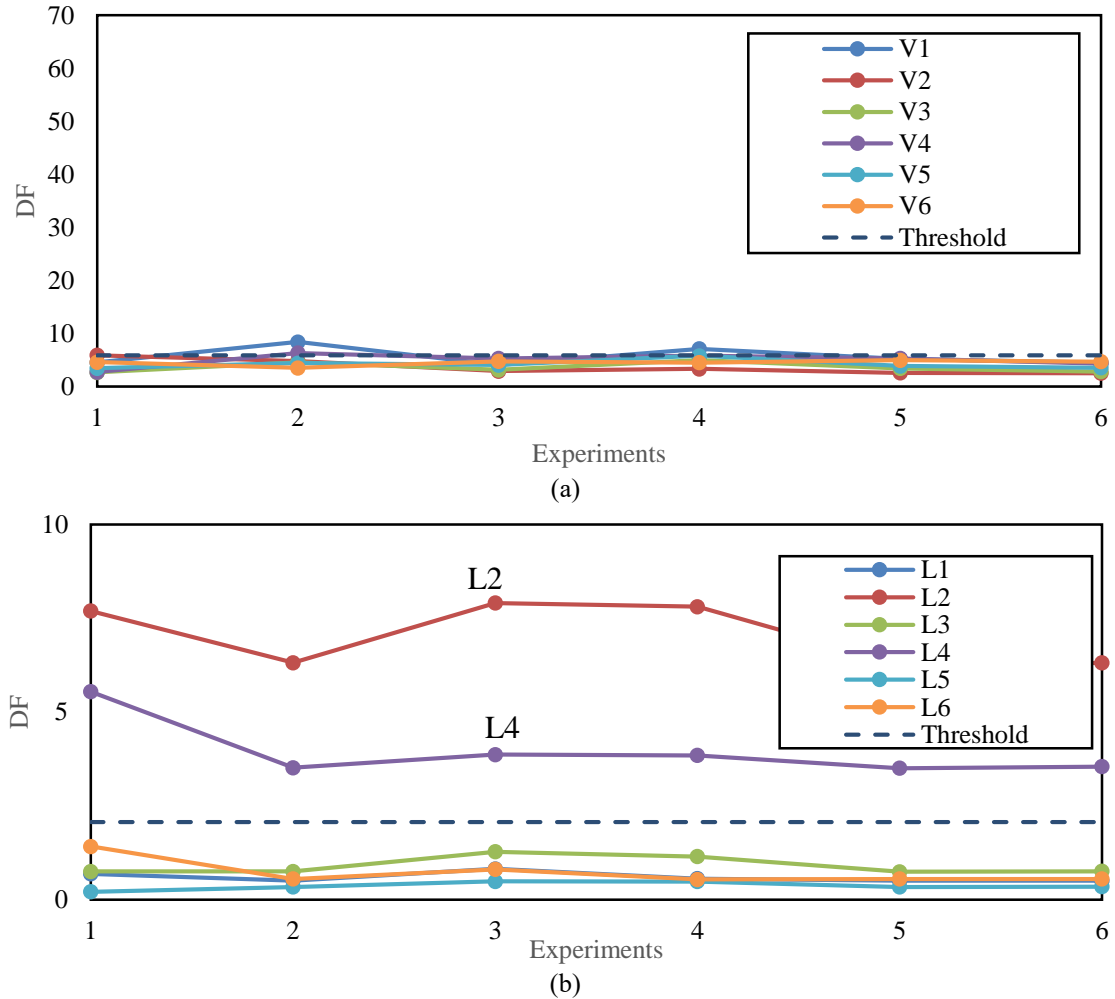


Fig. 10 Damage Features (DFs) for DC-B: (a) Vertical Cluster and (b) Longitudinal Cluster

5. Conclusions

This paper presents the results of experimental investigations performed based on a novel damage identification method for railway girder and truss bridges utilizing bridge acceleration response to operational loading. For experimental validation on a girder bridge, a simple steel deck is used. For truss bridge, a timber truss has been built which also included a steel deck. A controllable 2 axle vehicle is used to simulate vehicle loading. Since the method relies on the comparison of free vibration response from the baseline and the damaged bridge due to the passage of a single vehicle, it is suited to railway bridges. Trains usually pass over railway bridges following a schedule and usually, there is a time gap between each passage of a train. This makes the process of acquisition of useful free vibration data for railway bridges convenient, unlike other types of bridges (such as highway bridges) where vehicle movements are random and often multiple vehicles pass over the bridge at the same time.

The results presented in this study show reasonable agreement between predicted and expected damage features and demonstrate the potential of the proposed method. It is shown that the time-series analysis-based method under operational condition can detect and locate damage in the deck type bridge using only vertical acceleration response. For the truss bridge, a bi-axial sensor cluster system could provide information on damage on vertical and longitudinal elements using vertical and longitudinal acceleration responses, respectively. This method is presented for the instrumentation plan consisting of bi-axial accelerometers in each joint to facilitate element level damage localization. However, it is not practical to instrument all the joints especially if the bridge span is long. In such a situation, element level damage localization may not be possible.

It is acknowledged that fabrication errors might have occurred while building the test setup, especially in the truss bridge, since each element is manually sized and bolted. Even though the method is presented for railway bridges, during experiments, the railway track has not been included.

Finally, since the experimental tests are performed inside the laboratory, the effect of environmental condition changes on the measurement errors is also not considered in this study which could affect the performance of the method as it affects all damage detection methods in the literature. Currently, the author's research team is working on this topic extensively and developing methods using artificial neural networks to account for the environmental effects (Gu *et al.* 2011, Kostic and Güл 2017, Zhang *et al.* 2019).

Despite such limitations, the experimental results demonstrate that the proposed method has great promise for practical implementation and further research to address these limitations would improve the efficiency and robustness of the method for real-life application.

Acknowledgments

The study is funded by IC-IMPACTS (the India-Canada Centre for Innovative Multidisciplinary Partnerships to Accelerate Community Transformation and Sustainability), established through the Networks of Centres of Excellence of Canada.

References

- Azim, M.R. and Güл, M. (2020a), "Damage detection framework for truss railway bridges utilizing statistical analysis of operational strain response", *Struct. Control Health Monit.*, e2573. <https://doi.org/10.1002/stc.2573>.
- Azim, M.R. and Güл, M. (2020b), "Data-driven damage identification technique for truss railroad bridges utilizing principal component analysis of strain response", *Struct. Infrastruct. Eng.*, <https://doi.org/10.1080/15732479.2020.1785512>.
- Azim, M.R. and Güл, M. (2020c), "Damage detection of steel truss railway bridges using operational vibration data", *J. Struct. Eng. - ASCE*, **146**(3), 04020008. [https://doi.org/10.1061/\(ASCE\)ST.1943-541X.0002547](https://doi.org/10.1061/(ASCE)ST.1943-541X.0002547).
- Azim, M.R. and Güл, M. (2019), "Damage detection of steel girder railway bridges utilizing operational vibration response", *Struct. Control Health Monit.*, **26**(11), e2447. <https://doi.org/10.1002/stc.2447>.
- Beskhyroun, S., Oshima, T. and Mikami, S. (2010), "Wavelet-based technique for structural damage detection", *Struct. Control Health Monit.*, **17**, 473-494.
- Bowe, C., Quirke, P., Cantero, D. and O'Brien, E.J. (2015), "Drive-by structural health monitoring of railway bridges using train mounted accelerometers", *Proceedings of the 5th ECCOMAS Thematic Conference on Computational Methods in Structural Dynamics and Earthquake Engineering*. Greece.

- Brownjohn, J.M.W., Tjin, S.C., Tan, G.H. and Tan, B.L. (2004), "A structural health monitoring paradigm for civil infrastructure", *Proceedings of the 1st FIG International Symposium on Engineering Surveys for Construction Works and Structural Engineering*, Nottingham, UK.
- Celik, O., Terrell, T., Necati, C.F. and Güл, M. (2018), "Sensor clustering technique for practical structural monitoring and maintenance", *Struct. Monit. Maint.*, **5**(2), 273-295.
- CWC. (2020), "Visual grading of dimension lumber", *Canadian Wood Council*, Ottawa, Canada. <https://cwc.ca/how-to-build-with-wood/wood-products/lumber/grades/>
- Do, N.T., Mei, Q. and Gul, M. (2019), "Damage assessment of shear-type structures under varying mass effects", *Struct. Monit. Maint.*, **6**(3), 237-254. <https://doi.org/10.12989/smm.2019.6.3.237>.
- Farahani, R.V. and Penumadu, D. (2016), "Damage identification of a full-scale five-girder bridge using time-series analysis of vibration data", *Eng. Struct.*, **115**, 129-139.
- George, R.C., Posey, J., Gupta, A., Mukhopadhyay, S. and Mishra, S.K. (2017), "Damage detection in railway bridges under moving train load", *Proceedings of the Society for Experimental Mechanics Series. Model Validation and Uncertainty Quantification*, **3**, 349-354.
- Gonzalez, I. and Karoumi, R. (2015), "BWIM aided damage detection in bridges using machine learning", *J. Civil Struct. Health Monit.*, **5**, 715-725.
- Gu, J., Güл, M. and Wu, X. (2017), "Damage detection under varying temperature using Artificial Neural Networks", *J. Struct. Control Health Monit.*, **24**(11), e1998.
- Kim, C.W., Kitauchi, S., Chang, K.C., McGetrick, P.J., Sugiura, K. and Kawatani, M. (2014), "Structural damage diagnosis of steel truss bridges by outlier detection", *Proceedings of the 11th International Conference on Structural Safety and Reliability*, ICOSSAR, 4631-4638.
- Kopsaftopoulos, F.P. and Fassois, S.D. (2010), "Vibration based health monitoring for a lightweight truss structure: Experimental assessment of several statistical time series methods", *Mech. Syst. Signal Pr.*, **24**(7), 1977-1997.
- Kostic, B. and Güл, M. (2017), "Vibration based damage detection of bridges under varying temperature effects using time series analysis and artificial neural networks", *J. Bridge Eng. - ASCE*, **22**(10), 04017065.
- Lord Sensing Microstrain. (2019), <https://www.microstrain.com/wireless/g-link-200-oem>
- Lu, Z.R. and Liu, J.K. (2011), "Identification of both structural damages in bridge deck and vehicular parameters using measured dynamic responses", *Comput. Struct.*, **89**, 1397-1405.
- Mehrjou, M., Khaji, N., Moharrami, H. and Bahreininejad, A. (2008), "Damage detection of truss bridge joints using Artificial Neural Networks", *J. Exp. Syst. with Appl.*, **35**(3), 1122-1131.
- Mei, Q. and Güл, M. (2014), "Novel sensor clustering-based approach for simultaneous detection of stiffness and mass changes using output-only data", *J. Struct. Eng.*, **141**(10), 04014237. [https://doi.org/10.1061/\(ASCE\)ST.1943-541X.0001218](https://doi.org/10.1061/(ASCE)ST.1943-541X.0001218).
- Moreu, F., LaFave, J. and Spencer, B. (2012), "Structural health monitoring of railroad bridges – Research needs and preliminary results", *ASCE Structural Congress*, 2141-2152.
- Moreu, F., Jo, H., Li, J., Kim, R.E., Cho, S., Kimmle, A., Scola, S., Le, H., Spencer Jr., B.F. and LaFave, J.M. (2015), "Dynamic assessment of timber railroad bridges using displacements", *J. Bridge Eng. - ASCE*, **20**(10), 04014114.
- Moaveni, B., Hurlebus, S. and Moon, F. (2013), "Special issue on real-world applications of structural identification and health monitoring methodologies", *J. Struct. Eng.*, **139**(10), 1637-1638.
- PCB Piezotronics. (2019), <https://wwwpcb.com/products?model=393a03>
- Rytter, A. (1993), "Vibration Based Inspection of Civil Engineering Structures", Ph. D. dissertation; Aalborg University, Denmark.
- Sadhu, A., Goldack, A. and Narasimhan, S. (2015), "Ambient modal identification using multirank parallel factor decomposition", *Struct. Control Health Monit.*, **22**(4), 595-614.
- Scianna A.M. and Christenson R. (2009), "Probabilistic Structural Health Monitoring Method Applied to the Bridge Health Monitoring Benchmark Problem", *Transportation Research Record: Journal of Transportation Research Board*, 2131, 92-97.
- Scott, R.H., Banerji, P., Chikermane, S., Srinivasan, S., Basheer, P.A.M., Surre, F., Sun, T. and Grattan, K.T. V. (2013), "Commissioning and evaluation of a fiber-optic sensor system for bridge monitoring", *IEEE*

- Sensors J.*, **13** (7), 2555-2562.
- Siriwardane, S.C. (2015), “Vibration measurement-based simple technique for damage detection of truss bridges: a case study”, *J. Case Studies Eng. Fail. Anal.*, **4**, 50-58.
- Wang, L., Chan, T.H.T., Thambiratnam, D.P., Tan, A.C.C. and Cowled, C.J.L. (2012), “Correlation-based damage detection for complicated truss bridges using multi-layer genetic algorithms”, *Adv. Struct. Eng.*, **15**(5), 693-706.
- You, T., Gardoni, P., and Hurnlebaus, S. (2014), “Iterative damage index method for structural health monitoring”, *Struct. Monit. Maint.*, **1**(1), 89-110.
- Zhan, J.W., Xia, H., Chen, S.Y. and Roeck, G.D. (2011), “Structural damage identification for railway bridges based on train-induced bridge responses and sensitivity analysis”, *J. Sound Vib.*, **330**, 757-770.
- Zhang, H., Güл, M. and Kostic, B. (2019), “Eliminating temperature effects in damage detection for civil infrastructures using times series analysis and auto-associative neural networks”, *J. Aerosp. Eng.*, **32**(2), 04019001.

MK